Collins functions for pions from SIDIS and new e^+e^- data: A first glance at their transverse momentum dependence

M. Anselmino,[1,2] M. Boglione,[1,2] U. D'Alesio,[3,4] J. O. Gonzalez Hernandez,[1,2]
S. Melis,[1] F. Murgia,[4] and A. Prokudin[5]

[1]*Dipartimento di Fisica, Università di Torino, Via P. Giuria 1, I-10125 Torino, Italy*
[2]*INFN, Sezione di Torino, Via P. Giuria 1, I-10125 Torino, Italy*
[3]*Dipartimento di Fisica, Università di Cagliari, I-09042 Monserrato, Cagliari, Italy*
[4]*INFN, Sezione di Cagliari, C.P. 170, I-09042 Monserrato, Cagliari, Italy*
[5]*Division of Science, Penn State Berks, Reading, Pennsylvania 19610, USA*

(Received 23 October 2015; published 22 December 2015)

New data from the *BABAR* Collaboration, on azimuthal asymmetries measured in e^+e^- annihilations into pion pairs at $Q^2 = 112$ GeV^2, allow us to take the first, direct glance at the $p_\perp$ dependence of the Collins functions, in addition to their z dependence. These data, together with previous $e^+e^- \to h_1h_2$ Belle measurements and the available semi-inclusive deep inelastic scattering (SIDIS) data on the Collins asymmetry, are simultaneously analyzed in the framework of the generalized parton model, assuming two alternative Q^2 evolution schemes and exploiting two different parametrizations for the Collins functions. The corresponding results for the transversity distributions are presented. Analogous data, newly released by the BESIII Collaboration, on e^+e^- annihilations into pion pairs at the lower Q^2 of 13 GeV^2, offer the possibility to explore the sensitivity of these azimuthal correlations on transverse-momentum-dependent evolution effects.

DOI: 10.1103/PhysRevD.92.114023 PACS numbers: 13.88.+e, 13.60.-r, 13.85.Ni

I. INTRODUCTION

Our knowledge of the three-dimensional partonic structure of the nucleon in momentum space is encoded, at leading-twist, in eight transverse-momentum-dependent parton distribution functions (TMD-PDFs). They depend on two variables, the light-cone momentum fraction, x, of the parent nucleon's momentum carried by a parton and the parton transverse momentum, $\boldsymbol{k}_\perp$, with respect to the direction of the nucleon's motion. At a low resolution scale Q^2 the transverse momentum $\boldsymbol{k}_\perp$ may be associated with the intrinsic motion of confined partons inside the nucleon. For polarized nucleons and partons there is a further dependence on the spins of the nucleon and the parton. In addition, the QCD radiation of gluons induces a dependence on the scale Q^2 at which the nucleon is being explored.

Similarly, the hadronization process of a parton into the final hadron is encoded in the transverse-momentum-dependent parton fragmentation functions (TMD-FFs), which, in addition to spin depend on the light-cone momentum fraction, z, of the fragmenting parton carried by the hadron and the hadron transverse momentum, $\boldsymbol{p}_\perp$, with respect to the parton direction. For final spinless or unpolarized hadrons there are, at leading-twist, two independent TMD-FFs.

So far, among the polarized leading twist TMD-PDFs and TMD-FFs, the Sivers distribution [1,2] and the Collins fragmentation function [3] have clearly shown their non-negligible effects in several different experimental measurements. The former describes the correlation between the intrinsic momentum $\boldsymbol{k}_\perp$ of unpolarized partons and the parent nucleon transverse spin; as such, it must be related to parton orbital angular momentum. The latter describes the correlation between the transverse spin of a fragmenting quark and the transverse momentum $\boldsymbol{p}_\perp$ of the final produced hadron, typically a pion, with respect to the quark direction; as such, it reveals fundamental properties of the hadronization process. This paper is devoted to the study of the Collins functions.

The Collins fragmentation function can be studied in Semi-Inclusive Deep Inelastic Scattering (SIDIS) experiments, where it appears convoluted with the transversity distribution, and where, being dependent on $\boldsymbol{p}_\perp$, it induces a typical azimuthal modulation, the so-called Collins asymmetry. Clear signals of this asymmetry were observed experimentally, see Refs. [4–6]. The Collins fragmentation functions also induce azimuthal angular correlations between hadrons produced in opposite jets in e^+e^- annihilation [7,8]. Consequently, a simultaneous analysis of SIDIS and e^+e^- data allows the combined extraction of the transversity distribution and the Collins FFs [9–11].

Very recently, new data on the $e^+e^- \to h_1h_2X$ process have been published by the *BABAR* Collaboration, focusing on their z and $p_\perp$ dependence [12]. It is the first direct measurement of the transverse momentum dependence of an asymmetry, in e^+e^- processes, related to TMD functions. *BABAR* data benefit from very high statistics and offer, in addition to the z_1, z_2 distributions, data on the A_{12} asymmetry in bins of $(z_1, z_2, p_{\perp 1}, p_{\perp 2})$ and in bins of $p_{\perp 1}$

and $p_{\perp 2}$, where $p_{\perp 1}$ and $p_{\perp 2}$ are the transverse momenta of the final hadrons with respect to the thrust axis. Moreover, *BABAR* measures the A_0 asymmetry as a function of P_{1T}, the transverse momentum of the final hadron h_1 with respect to the plane which contains both the e^+e^- pair and the other final hadron, h_2, in the e^+e^- c.m. frame. Information on the transverse momentum dependence of the asymmetries thus allows a first glance at the dependence of the Collins FFs on the transverse momentum, $p_\perp$.

The explicit dependence of the TMDs on their corresponding momentum fractions x or z is relatively easy to access, as most measured observables (cross sections, multiplicities, asymmetries) are given as functions of x or z, although still in a limited range. Instead, the transverse momentum dependence is much more involved, as $k_\perp$ and $p_\perp$ are never observed directly but only through convolutions. Asymmetries alone are not sufficient for a complete study of the Collins transverse momentum dependence, as they require the knowledge of the unpolarized TMD fragmentation functions, which appear in the denominator of the asymmetry. Information on the unpolarized FFs have historically been extracted from SIDIS processes where, unfortunately, the $k_\perp$ and $p_\perp$ dependences are strongly correlated and cannot be disentangled unambiguously. For a direct extraction of the $p_\perp$ dependence of the unpolarized FFs one would need to measure, for example, transverse-momentum-dependent cross sections or multiplicities in $e^+e^- \to h_1 h_2 X$ processes, which would, finally, allow the extraction of the $p_\perp$ dependence of the Collins function from e^+e^- asymmetries. Although the present study cannot deliver an absolute determination of the Collins function, our analysis of the new *BABAR* measurements allows to obtain the relative TMD behavior of the Collins function with respect to that of the unpolarized TMD–FF.

In this paper we adopt a phenomenological model for TMD–PDFs and FFs in a scheme where the cross section is written as the convolution of two TMDs with the corresponding partonic cross section. Moreover, we assume that the TMD longitudinal and transverse degrees of freedom factorize. The z-dependent part of our TMDs evolves in Q^2 while the transverse-momentum-dependent part is Q^2 independent. This model, sometimes called the generalized parton model (GPM), has proven to work surprisingly well, allowing to describe a wide variety of observables: from the SIDIS unpolarized multiplicities [13–15], to SIDIS Sivers and Collins effects [11,16,17] up to the most intriguing spin asymmetries in inclusive hadron production [18,19].

Proper treatment of TMDs would require the use of TMD evolution [20]. In fact, one expects that, as Q^2 grows, gluon radiations will change the functional form of the $k_\perp$ and $p_\perp$ dependence: in particular, the widths of the TMDs will generically grow with Q^2. The corresponding evolution equations are the so-called Collins-Soper (CS) equations [21,22]. Recently, evolution equations have been formulated for unpolarized TMD functions directly [20,23–25]. Polarized TMDs, in particular the Collins FFs, were shown to have similar evolution equations [25] and the first analysis of the SIDIS and e^+e^- data including TMD evolution was presented in Ref. [26]. The results of Ref. [26] are similar to the GPM model results published in Ref. [11].

The TMD approach is valid in the region in which $q_T \ll Q$, where $q_T \simeq P_T/z$ and Q^2 are the transverse momentum and the virtuality of the probing photon, respectively. Available SIDIS data cover the region from low to moderate Q^2. For instance the average values of Q^2 of the SIDIS data considered in the present analysis are between 2.4 and 3.2 GeV^2, while the typical transverse momentum P_T of the final hadron is between 0.1 and 1.5 GeV. Clearly, in this region, it is difficult to guarantee $q_T \ll Q$. It is then crucial to test the validity of the TMD approach in this range of Q^2 and q_T by comparing our results and those obtained by applying a TMD evolution scheme [26] to the available experimental data.

In principle e^+e^- Collins asymmetry data, which correspond to a much larger Q^2, allow the application of the TMD evolution scheme in its range of validity. However, the observables we are analyzing are, in general, ratios or double ratios of cross sections, where strong cancellations of TMD evolution effects can occur. Therefore, we have to understand whether soft gluon emissions, typical of TMD evolution, affect the Collins asymmetries, and whether we can unambiguously observe any explicit Q^2 dependence in the presently available data. This might also help to better determine the universal, nonperturbative part of TMD evolution [27,28]. Having no Q^2 evolution in the transverse momentum distribution, our model could be considered as a benchmark for this kind of studies.

Almost at completion of our paper new results from the BESIII Collaboration have appeared [29]. They definitely confirm the need for nonvanishing Collins functions; in addition, they present the very interesting feature of being at much lower Q^2 values with respect to Belle and *BABAR* data. We do not include them in our fitting procedure, but rather we will compare our determination of the Collins functions with these new results, and explore the sensitivity of these azimuthal correlations on Q^2-dependent effects.

The purpose of this paper is twofold. First, we would like to test the GPM against the new e^+e^- data, both from *BABAR* and BESIII Collaborations, and see whether the newest data put limitations on the region of applicability of our model. Second, we would like to study the $p_\perp$ dependence of the pion Collins functions.

We only consider here pion production. The *BABAR* Collaboration has recently also measured azimuthal correlations for pion-kaon and kaon-kaon pairs produced in e^+e^- annihilations [30]. They allow the first ever extraction of the kaon Collins function and will be considered in a forthcoming paper.

The paper is organized as follows. In Sec. II we briefly recall the formalism used in our analysis, while in Sec. III

we discuss our of Belle [31,32], *BABAR* [12], HERMES [4] and COMPASS [6,33] results and present our extraction of the valence quark transversity distributions and of the pion Collins functions. In Sec. IV we study how our choice of parametrization for the Collins function affects the results of our fit and study its dependence on the chosen evolution scheme. The newly released, low energy, BESIII data will be discussed in Sec. V. Final comments, including some considerations on the role of TMD evolution in phenomenological analyses of asymmetries, will be given in Sec. VI, together with our conclusions.

II. FORMALISM

Our strategy for the extraction of the TMD transversity and Collins functions is based on a simultaneous best fit of SIDIS and $e^+e^- \to h_1 h_2 X$ experimental data. We only summarize here the basic formalism used throughout the paper; all details can be found in Refs. [9,11,34] to which we refer for notations, kinematical variables, and for the definition of the azimuthal angles which appear in the following equations.

A. SIDIS

In SIDIS processes, at $\mathcal{O}(k_\perp/Q)$, the $\sin(\phi_h+\phi_S)$ moment of the measured spin asymmetry A_{UT} [34,35], is proportional to the spin-dependent part of the fragmentation function of a transversely polarized quark, encoded in the Collins function, $\Delta^N D_{h/q^\uparrow}(z,p_\perp) = (2p_\perp/zm_h)H_1^{\perp q}(z,p_\perp)$ [36], convoluted with the TMD transversity distribution $\Delta_T q(x,k_\perp)$ [9]:

$$A_{UT}^{\sin(\phi_h+\phi_S)} = \frac{\sum_q e_q^2 \int d\phi_h d\phi_S d^2\boldsymbol{k}_\perp \Delta_T q(x,k_\perp)\frac{d(\Delta\hat{\sigma})}{dy}\Delta^N D_{h/q^\uparrow}(z,p_\perp)\sin(\phi_S+\varphi+\phi_q^h)\sin(\phi_h+\phi_S)}{\sum_q e_q^2 \int d\phi_h d\phi_S d^2\boldsymbol{k}_\perp f_{q/p}(x,k_\perp)\frac{d\hat{\sigma}}{dy}D_{h/q}(z,p_\perp)}. \tag{1}$$

The above equation further simplifies when adopting a Gaussian and factorized parametrization for the TMDs. In particular for the unpolarized parton distribution and fragmentation functions we assume

$$f_{q/p}(x,k_\perp) = f_{q/p}(x)\frac{e^{-k_\perp^2/\langle k_\perp^2\rangle}}{\pi\langle k_\perp^2\rangle}, \tag{2}$$

$$D_{h/q}(z,p_\perp) = D_{h/q}(z)\frac{e^{-p_\perp^2/\langle p_\perp^2\rangle}}{\pi\langle p_\perp^2\rangle}. \tag{3}$$

For the integrated parton distribution and fragmentation functions, $f_{q/p}(x)$ and $D_{h/q}(z)$, we use respectively the GRV98LO PDF set [37] and the de Florian, Sassot and Stratmann (DSS) FF set [38]. This choice is dictated by the fact that GRV98LO is the only PDF set with an initial scale, Q_0, low enough to accommodate all HERMES data points, including those at the lowest values of Q^2. We have checked that different choices of distribution and fragmentation function sets hardly influence the outcome of our analysis. The Gaussian widths are fixed to the values obtained by fitting HERMES SIDIS multidimensional multiplicities in Ref. [14]:

$$\langle k_\perp^2\rangle = 0.57\ \text{GeV}^2 \quad \langle p_\perp^2\rangle = 0.12\ \text{GeV}^2. \tag{4}$$

Notice that these values were obtained using the unpolarized CTEQ6LO PDFs [39], rather than the GRV98LO PDFs, adopted here; again, we have explicitly checked that using the GRV98LO PDFs in fitting the multidimensional multiplicities would not change the above results.

These values are different from those obtained and adopted in previous analyses [9,11,34]. The determination of the separate values of $\langle k_\perp^2\rangle$ and $\langle p_\perp^2\rangle$ from SIDIS data is still rather uncertain, and we have preferred here to choose the most recently obtained values, which give a good fit [14] of the unpolarized multiplicities.

For the transversity distribution, $\Delta_T q(x,k_\perp)$, and the Collins FF, $\Delta^N D_{h/q^\uparrow}(z,p_\perp)$, we adopt the following factorized shapes [9]:

$$\Delta_T q(x,k_\perp;Q^2) = \Delta_T q(x,Q^2)\frac{e^{-k_\perp^2/\langle k_\perp^2\rangle_T}}{\pi\langle k_\perp^2\rangle_T}, \tag{5}$$

$$\Delta^N D_{h/q^\uparrow}(z,p_\perp;Q^2) = \tilde{\Delta}^N D_{h/q^\uparrow}(z,Q^2)h(p_\perp)\frac{e^{-p_\perp^2/\langle p_\perp^2\rangle}}{\pi\langle p_\perp^2\rangle}, \tag{6}$$

where $\Delta_T q(x)$ is the integrated transversity distribution and $\tilde{\Delta}^N D_{h/q^\uparrow}(z)$ is the z-dependent part of the Collins function. In order to easily implement the proper positivity bounds, these functions are written, at the initial scale Q_0^2, as [9]

$$\Delta_T q(x,Q_0^2) = \mathcal{N}_q^T(x,Q_0^2)\frac{1}{2}[f_{q/p}(x,Q_0^2)+\Delta q(x,Q_0^2)] \tag{7}$$

$$\tilde{\Delta}^N D_{h/q^\uparrow}(z,Q_0^2) = 2\mathcal{N}_q^C(z,Q_0^2)D_{h/q}(z,Q_0^2). \tag{8}$$

They are then evolved up to the proper value of Q^2. For $\Delta_T q(x,Q^2)$ we employ a transversity DGLAP kernel and the evolution is performed by an appropriately modified

HOPPET code [40]. The Soffer bound is built in by using the GRV98LO [37] and GRSV2000 [41] PDF sets at the input scale of $Q_0^2 = 1\ \mathrm{GeV}^2$, with $\alpha_s(Q_0) = 0.44$ calculated according to the GRV98 LO scheme. In this analysis, we use a simplified model which implies no Q^2 dependence in the $p_\perp$ distribution. As the Collins function in our parametrization is proportional to the unpolarized fragmentation function, see Eqs. (6) and (8), we assume that the only scale dependence is contained in $D(z, Q^2)$, which is evolved with an unpolarized DGLAP kernel, while $\mathcal{N}_q^C$ does not evolve with Q^2. This is equivalent to assuming that the ratio $\tilde{\Delta}^N D(z, Q^2)/D(z, Q^2)$ is constant in Q^2. Throughout the paper, we will refer to this choice as the "standard" evolution scheme.

The function $h(p_\perp)$, defined as [9]

$$h(p_\perp) = \sqrt{2e}\,\frac{p_\perp}{M_C}\,e^{-p_\perp^2/M_C^2}, \tag{9}$$

allows for a possible modification of the $p_\perp$ Gaussian width of the Collins function with respect to the unpolarized FF; for the TMD transversity distribution, instead, we assume the same Gaussian width as for the unpolarized TMD, $\langle k_\perp^2\rangle_T = \langle k_\perp^2\rangle$.

We parametrize $\mathcal{N}_q^T(x)$ as

$$\mathcal{N}_q^T(x) = N_q^T x^\alpha (1-x)^\beta \frac{(\alpha+\beta)^{\alpha+\beta}}{\alpha^\alpha \beta^\beta} \quad (q = u_v, d_v), \tag{10}$$

where $-1 \le N_q^T \le +1$, α and β are free parameters of the fit. Thus, the transversity distributions depend on a total of four parameters $(N_{u_v}^T, N_{d_v}^T, \alpha, \beta)$.

For the Collins function, as in previous papers [9,11], we distinguish between favored and disfavored fragmentations. The favored contribution is parametrized as

$$\mathcal{N}_{\mathrm{fav}}^C(z) = N_{\mathrm{fav}}^C z^\gamma (1-z)^\delta \frac{(\gamma+\delta)^{\gamma+\delta}}{\gamma^\gamma \delta^\delta}, \tag{11}$$

where $-1 \le N_{\mathrm{fav}}^C \le +1$, γ and δ are free parameters of the fit. Differently from what we did in the past, we do not assume the same functional shape for favored and disfavored Collins functions. In a first attempt we chose for $\mathcal{N}_{\mathrm{dis}}^C$ a parametrization analogous to that shown in Eq. (11), letting the fit free to choose different γ and δ parameters. It turned out that, for the disfavored Collins function, the best-fit values of γ and δ were very close or compatible with zero. One should also notice that, with the presently available SIDIS and e^+e^- data, the disfavored Collins function is largely undetermined. Consequently, also in order to reduce the number of parameters, we simply choose

$$\mathcal{N}_{\mathrm{dis}}^C(z) = N_{\mathrm{dis}}^C. \tag{12}$$

Thus, we have a total of five free parameters for the Collins functions $(M_C, N_{\mathrm{fav}}^C, N_{\mathrm{dis}}^C, \gamma, \delta)$. Notice that, although present data are still unable to tightly constrain the disfavored Collins function, it clearly turns out that choosing independent parametrizations for $\mathcal{N}_{\mathrm{fav}}^C(z)$ and $\mathcal{N}_{\mathrm{dis}}^C(z)$ definitely improves the quality of the fit.

Using Eqs. (2), (3), (5), (6) in Eq. (1), we obtain the following expression for $A_{UT}^{\sin(\phi_h+\phi_S)}$:

$$A_{UT}^{\sin(\phi_h+\phi_S)} = \frac{\sqrt{2e}\,\frac{P_T}{M_C}\,\frac{\langle p_\perp^2\rangle_C^2}{\langle p_\perp^2\rangle}\,\frac{e^{-P_T^2/\langle P_T^2\rangle_C}}{\langle P_T^2\rangle_C^2}\,\frac{1-y}{sxy^2}\sum_q e_q^2 \Delta_T q(x)\tilde{\Delta}^N D_{h/q^\uparrow}(z)}{\frac{e^{-P_T^2/\langle P_T^2\rangle}}{\langle P_T^2\rangle}\,\frac{[1+(1-y)^2]}{sxy^2}\sum_q e_q^2 f_{q/p}(x) D_{h/q}(z)}, \tag{13}$$

with

$$\langle p_\perp^2\rangle_C = \frac{M_C^2\langle p_\perp^2\rangle}{M_C^2 + \langle p_\perp^2\rangle}$$
$$\langle P_T^2\rangle_{(C)} = \langle p_\perp^2\rangle_{(C)} + z^2\langle k_\perp^2\rangle. \tag{14}$$

B. $e^+e^- \to h_1 h_2 X$ processes

Independent information on the Collins functions can be obtained in unpolarized e^+e^- processes, by looking at the azimuthal correlations of hadrons produced in opposite jets [7]. The Belle Collaboration [8,31,32] and, more recently, the *BABAR* Collaboration [12] have measured azimuthal hadron-hadron correlations for inclusive charged pion production in $e^+e^- \to \pi\pi X$ processes, which, involving the convolution of two Collins functions, can be interpreted as a direct measure of the Collins effect.

Two methods have been adopted in the experimental analysis of the Belle and *BABAR* data [7,9,12,31]:

(1) In the "thrust-axis method" the jet thrust axis, in the e^+e^- c.m. frame, fixes the $\hat{z}$ direction and the $e^+e^- \to q\bar{q}$ scattering defines the $\hat{x}z$ plane; φ_1 and φ_2 are the azimuthal angles of the two hadrons around the thrust axis, while θ is the angle between the lepton direction and the thrust axis. In this reference frame, with unpolarized leptons, the cross section can be written as [9]

$$\frac{d\sigma^{e^+e^-\to h_1h_2X}}{dz_1dz_2p_{\perp1}dp_{\perp1}p_{\perp2}dp_{\perp2}d\cos\theta d(\varphi_1+\varphi_2)} = \frac{3\pi^2\alpha^2}{s}\sum_q e_q^2\Big\{(1+\cos^2\theta)D_{h_1/q}(z_1,p_{\perp1}) \times D_{h_2/\bar q}(z_2,p_{\perp2}) + \frac{1}{4}\sin^2\theta\Delta^N D_{h_1/q^\uparrow}(z_1,p_{\perp1})\Delta^N D_{h_2/\bar q^\uparrow}(z_2,p_{\perp2}) \times\cos(\varphi_1+\varphi_2)\Big\}. \tag{15}$$

Until very recently, only data on the z dependence were available, while $p_{\perp1}$ and $p_{\perp2}$ were integrated out. However, in 2014 the *BABAR* Collaboration has released a new analysis in which multidimensional data are presented [12]. This represents the first direct measurement of the dependence of the Collins function on the intrinsic transverse momenta $p_{\perp1}$ and $p_{\perp2}$.

By normalizing Eq. (15) to the azimuthal averaged cross section,

$$\langle d\sigma\rangle \equiv \frac{1}{2\pi}\frac{d\sigma^{e^+e^-\to h_1h_2X}}{dz_1dz_2p_{\perp1}dp_{\perp1}p_{\perp2}dp_{\perp2}d\cos\theta} = \frac{3\pi^2\alpha^2}{s}\sum_q e_q^2(1+\cos^2\theta)D_{h_1/q}(z_1,p_{\perp1}) \times D_{h_2/\bar q}(z_2,p_{\perp2}), \tag{16}$$

one has

$$R_{12}(z_1,z_2,p_{\perp1},p_{\perp2},\theta,\varphi_1+\varphi_2) \equiv \frac{1}{\langle d\sigma\rangle}\frac{d\sigma^{e^+e^-\to h_1h_2X}}{dz_1dz_2p_{\perp1}dp_{\perp1}p_{\perp2}dp_{\perp2}d\cos\theta d(\varphi_1+\varphi_2)} = 1+\frac{1}{4}\frac{\sin^2\theta}{1+\cos^2\theta}\cos(\varphi_1+\varphi_2) \times\frac{\sum_q e_q^2\Delta^N D_{h_1/q^\uparrow}(z_1,p_{\perp1})\Delta^N D_{h_2/\bar q^\uparrow}(z_2,p_{\perp2})}{\sum_q e_q^2 D_{h_1/q}(z_1,p_{\perp1})D_{h_2/\bar q}(z_2,p_{\perp2})}. \tag{17}$$

To eliminate false asymmetries, the Belle and *BABAR* Collaborations consider the ratio of unlike sign $(\pi^+\pi^- + \pi^-\pi^+)$ to like sign $(\pi^+\pi^+ + \pi^-\pi^-)$ or charged $(\pi^+\pi^+ + \pi^+\pi^- + \pi^-\pi^+ + \pi^-\pi^-)$ pion pair production, denoted, respectively, with indices U, L and C. For example, in the case of unlike- to like-pair production, one has

$$\frac{R_{12}^U}{R_{12}^L} = \frac{1+\frac{1}{4}\cos(\varphi_1+\varphi_2)\frac{\sin^2\theta}{1+\cos^2\theta}P_U}{1+\frac{1}{4}\cos(\varphi_1+\varphi_2)\frac{\sin^2\theta}{1+\cos^2\theta}P_L} \simeq 1+\frac{1}{4}\cos(\varphi_1+\varphi_2)\frac{\sin^2\theta}{1+\cos^2\theta}(P_U-P_L) \equiv 1+\cos(\varphi_1+\varphi_2)A_{12}^{UL}(z_1,z_2,p_{\perp1},p_{\perp2},\theta), \tag{18}$$

with

$$P_U \equiv \frac{(P_U)_N}{(P_U)_D} = \frac{\sum_q e_q^2[\Delta^N D_{\pi^+/q^\uparrow}(z_1,p_{\perp1})\Delta^N D_{\pi^-/\bar q^\uparrow}(z_2,p_{\perp2}) + \Delta^N D_{\pi^-/q^\uparrow}(z_1,p_{\perp1})\Delta^N D_{\pi^+/\bar q^\uparrow}(z_2,p_{\perp2})]}{\sum_q e_q^2[D_{\pi^+/q}(z_1,p_{\perp1})D_{\pi^-/\bar q}(z_2,p_{\perp2}) + D_{\pi^-/q}(z_1,p_{\perp1})D_{\pi^+/\bar q}(z_2,p_{\perp2})]}, \tag{19}$$

$$P_L \equiv \frac{(P_L)_N}{(P_L)_D} = \frac{\sum_q e_q^2[\Delta^N D_{\pi^+/q^\uparrow}(z_1,p_{\perp1})\Delta^N D_{\pi^+/\bar q^\uparrow}(z_2,p_{\perp2}) + \Delta^N D_{\pi^-/q^\uparrow}(z_1,p_{\perp1})\Delta^N D_{\pi^-/\bar q^\uparrow}(z_2,p_{\perp2})]}{\sum_q e_q^2[D_{\pi^+/q}(z_1,p_{\perp1})D_{\pi^+/\bar q}(z_2,p_{\perp2}) + D_{\pi^-/q}(z_1,p_{\perp1})D_{\pi^-/\bar q}(z_2,p_{\perp2})]}, \tag{20}$$

$$A_{12}^{UL}(z_1,z_2,p_{\perp1},p_{\perp2},\theta) = \frac{1}{4}\frac{\sin^2\theta}{1+\cos^2\theta}(P_U-P_L). \tag{21}$$

Similarly, for $A_{12}^{UC}(z_1,z_2,p_{\perp1},p_{\perp2},\theta)$ we have

$$A_{12}^{UC}(z_1,z_2,p_{\perp1},p_{\perp2},\theta) = \frac{1}{4}\frac{\sin^2\theta}{1+\cos^2\theta}(P_U-P_C), \tag{22}$$

where

$$P_C = \frac{(P_U)_N+(P_L)_N}{(P_U)_D+(P_L)_D}. \tag{23}$$

Notice that, in order to obtain the $p_\perp$ integrated asymmetries where only the z_1, z_2 dependence is preserved, in Eqs. (19) and (20) we first integrate numerators and denominators separately over $p_{\perp1}$ and $p_{\perp2}$, and *then* we take ratios.

As said before, for fitting purposes it is convenient to introduce favored and disfavored fragmentation functions, that is [see Eqs. (6) and (8)]

$$\frac{\Delta^N D_{\pi^+/u^\uparrow,\bar{d}^\uparrow}(z,p_\perp)}{D_{\pi^+/u,\bar{d}}(z)} = \frac{\Delta^N D_{\pi^-/d^\uparrow,\bar{u}^\uparrow}(z,p_\perp)}{D_{\pi^-/d,\bar{u}}(z)} = 2\mathcal{N}^C_{\rm fav}(z)h(p_\perp)\frac{e^{-p_\perp^2/\langle p_\perp^2\rangle}}{\pi\langle p_\perp^2\rangle} \tag{24}$$

$$\frac{\Delta^N D_{\pi^+/d^\uparrow,\bar{u}^\uparrow}(z,p_\perp)}{D_{\pi^+/d,\bar{u}}(z)} = \frac{\Delta^N D_{\pi^-/u^\uparrow,\bar{d}^\uparrow}(z,p_\perp)}{D_{\pi^-/u,\bar{d}}(z)} = \frac{\Delta^N D_{\pi^\pm/s^\uparrow,\bar{s}^\uparrow}(z,p_\perp)}{D_{\pi^\pm/s,\bar{s}}(z)} = 2\mathcal{N}^C_{\rm dis}(z)h(p_\perp)\frac{e^{-p_\perp^2/\langle p_\perp^2\rangle}}{\pi\langle p_\perp^2\rangle}. \tag{25}$$

(2) In the "hadronic-plane method," one of the produced hadrons (h_2 in our case) identifies the $\hat{z}$ direction and the $\hat{xz}$ plane is determined by the lepton and the h_2 directions; the other relevant plane is determined by $\hat{z}$ and the direction of the other observed hadron, h_1, at an angle ϕ_1 with respect to the $\hat{xz}$ plane. Here θ_2 is the angle between h_2 and the e^+e^- direction.

In this reference frame, the elementary process $e^+e^- \to q\bar{q}$ does not occur in the $\hat{xz}$ plane, and thus the helicity scattering amplitudes involve an azimuthal phase φ_2. The analogue of Eq. (15) now reads

$$\frac{d\sigma^{e^+e^-\to h_1h_2X}}{dz_1dz_2d^2p_{\perp1}d^2p_{\perp2}d\cos\theta_2} = \frac{3\pi\alpha^2}{2s}\sum_q e_q^2\Big\{(1+\cos^2\theta_2)D_{h_1/q}(z_1,p_{\perp1}) \times D_{h_2/\bar{q}}(z_2,p_{\perp2}) + \frac{1}{4}\sin^2\theta_2\Delta^N D_{h_1/q^\uparrow}(z_1,p_{\perp1})\Delta^N D_{h_2/\bar{q}^\uparrow}(z_2,p_{\perp2}) \times \cos(2\varphi_2+\phi_q^{h_1})\Big\}, \tag{26}$$

where $\phi_q^{h_1}$ is the azimuthal angle of the detected hadron h_1 around the direction of the parent fragmenting quark, q. In other words, $\phi_q^{h_1}$ is the azimuthal angle of $\boldsymbol{p}_{\perp1}$ in the helicity frame of q. It can be expressed in terms of the integration variables we are using, $\boldsymbol{p}_{\perp2}$ and $\boldsymbol{P}_{1T}$, the transverse momentum of the h_1 hadron. At lowest order in $p_\perp/(z\sqrt{s})$, we have

$$\cos\phi_q^{h_1} = \frac{P_{1T}}{p_{\perp1}}\cos(\phi_1-\varphi_2) - \frac{z_1}{z_2}\frac{p_{\perp2}}{p_{\perp1}}, \tag{27}$$

$$\sin\phi_q^{h_1} = \frac{P_{1T}}{p_{\perp1}}\sin(\phi_1-\varphi_2). \tag{28}$$

The integration over $\boldsymbol{p}_{\perp2}$ is performed explicitly, using the parametrization of the Collins function given in Eq. (6), while, as $\boldsymbol{p}_{\perp1} = \boldsymbol{P}_1 - z_1\boldsymbol{q}_1$, we can replace $d^2\boldsymbol{p}_{\perp1}$ with $d^2\boldsymbol{P}_{1T}$. We obtain

$$\frac{d\sigma^{e^+e^-\to h_1h_2X}}{dz_1dz_2d^2\boldsymbol{P}_{1T}d\cos\theta_2} = \frac{3\pi\alpha^2}{2s}\{D_{h_1h_2} + N_{h_1h_2}\cos(2\phi_1)\}, \tag{29}$$

where

$$D_{h_1h_2} = (1+\cos^2\theta_2)\sum_q e_q^2 D_{h_1/q}(z_1) \times D_{h_2/\bar{q}}(z_2)\frac{\exp\left[-\frac{P_{1T}^2}{\langle\tilde{p}_\perp^2\rangle}\right]}{\pi\langle\tilde{p}_\perp^2\rangle}, \tag{30}$$

$$N_{h_1h_2} = \frac{1}{4}\frac{z_1z_2}{z_1^2+z_2^2}\sin^2\theta_2\sum_q e_q^2\tilde{\Delta}^N D_{h_1/q^\uparrow}(z_1) \times \tilde{\Delta}^N D_{h_2/\bar{q}^\uparrow}(z_2)\frac{2eP_{1T}^2}{\tilde{M}_C^2+\langle\tilde{p}_\perp^2\rangle}\frac{\exp\left[-\frac{P_{1T}^2}{\tilde{M}_C^2}-\frac{P_{1T}^2}{\langle\tilde{p}_\perp^2\rangle}\right]}{\pi\langle\tilde{p}_\perp^2\rangle}, \tag{31}$$

and

$$\tilde{M}_C^2 = M_C^2\frac{(z_1^2+z_2^2)}{z_2^2}, \qquad \langle\tilde{p}_\perp^2\rangle = \langle p_\perp^2\rangle\frac{(z_1^2+z_2^2)}{z_2^2}. \tag{32}$$

The unlike, like and charged combinations are

$$D^U = D_{\pi^+\pi^-} + D_{\pi^-\pi^+} \quad N^U = N_{\pi^+\pi^-} + N_{\pi^-\pi^+} \tag{33}$$

$$D^L = D_{\pi^+\pi^+} + D_{\pi^-\pi^-} \quad N^L = N_{\pi^+\pi^+} + N_{\pi^-\pi^-} \tag{34}$$

$$D^C = D^U + D^L \quad N^C = N^U + N^L, \tag{35}$$

so that

$$P_0^{U,L,C} = \frac{N^{U,L,C}}{D^{U,L,C}}, \tag{36}$$

and finally

$$R_0^{U,L,C} = 1 + P_0^{U,L,C}\cos(2\phi_1). \tag{37}$$

As in the previous case, we can build ratios of unlike/like and unlike/charged asymmetries,

$$\frac{R_0^U}{R_0^{L(C)}} = \frac{1 + P_0^U \cos(2\phi_1)}{1 + P_0^{L(C)} \cos(2\phi_1)} \simeq 1 + (P_0^U - P_0^{L(C)}) \cos(2\phi_1) \equiv 1 + \cos(2\phi_1) A_0^{UL(C)}, \quad (38)$$

which can then be directly compared to the experimental measurements.

III. BEST FIT OF SIDIS AND e^+e^- DATA: TRANSVERSITY DISTRIBUTIONS, COLLINS FUNCTIONS AND COMPARISON WITH DATA

We can now perform a best fit of the data on $A_{UT}^{\sin(\phi_h+\phi_S)}$ from HERMES and COMPASS and of the data on $A_0^{UL,C}$, from the Belle and *BABAR* Collaborations. As anticipated above, we will not exploit the $A_{12}^{UL,C}$ data in our fit, but only use them as a consistency check of our results. In our fit—we shall refer to it as the "reference" fit—these asymmetries, given in Eqs. (13) and (38), are expressed in terms of the transversity and the Collins functions, parametrized as in Eqs. (2)–(12), and evolved according to the "standard" evolution scheme [see comments after Eq. (8)].

The transversity and the Collins functions depend on the free parameters $\alpha, \beta, \gamma, \delta, N_q^T, N_q^C$ and M_C. Following Ref. [9] we assume the exponents α, β and the mass scale M_C to be flavor independent. Here we consider the transversity distributions only for u and d valence quarks (with the two free parameters $N_{u_v}^T$ and $N_{d_v}^T$). The favored Collins function is fixed by the flavor-independent exponents γ and δ, and by $N_{\rm fav}^C$, while the disfavored Collins function is determined by the sole parameter $N_{\rm dis}^C$ [see comments before Eq. (12)]. This makes a total of nine parameters to be fixed with a best-fit procedure. Notice that while in the present analysis we can safely neglect any flavor dependence of the parameter β (which is anyway very loosely constrained by SIDIS data), this issue could play a significant role in other studies, like the determination of the tensor charge [18].

Table I reports the values of the parameters as determined by the best-fitting procedure, while in Table II we summarize the total χ^2 s of the fit and the χ^2 contributions corresponding to SIDIS and e^+e^- experiments separately. As one can see, this fit is very good. All data sets are very well reproduced, as shown in Figs. 1–5. The statistical errors shown in Table I and the bands in Figs. 1–15 are obtained by sampling 1850 sets of parameters corresponding to a χ^2 value in the range between $\chi^2_{\rm min}$ and $\chi^2_{\rm min} + \Delta\chi^2$, as explained in Ref. [16]. The value of $\Delta\chi^2$ corresponds to 95.45% confidence level for nine parameters; in this case we have $\Delta\chi^2 = 17.2$.

TABLE I. Best reference fit values of the nine free parameters fixing the u and d valence quark transversity distribution functions and the favored and disfavored Collins fragmentation functions, as obtained by fitting simultaneously HERMES and COMPASS data on the Collins asymmetry and Belle and *BABAR* data on A_0^{UL} and A_0^{UC}.

$N_{u_v}^T = 0.61^{+0.39}_{-0.23}$	$N_{d_v}^T = -1.00^{+1.86}_{-0.00}$
$\alpha = 0.70^{+1.31}_{-0.63}$	$\beta = 1.80^{+7.60}_{-1.80}$
$N_{\rm fav}^C = 0.90^{+0.09}_{-0.34}$	$N_{\rm dis}^C = -0.37^{+0.05}_{-0.05}$
$\gamma = 2.02^{+0.83}_{-0.33}$	$\delta = 0.00^{+0.42}_{-0.00}$
$M_C^2 = 0.28^{+0.20}_{-0.09}$ GeV^2	

TABLE II. Contributions of each individual set of fitted data to the total χ^2 of our reference fit. The upper part of the table refers to e^+e^- data. Here we show the χ^2s obtained for the Belle and *BABAR* A_0^{UL} and A_0^{UC} asymmetries as functions of z_1 and z_2 (integrated over the hadronic transverse momentum P_{1T}) and as a functions of P_{1T} (integrated over z_1 and z_2). The second part refers to SIDIS measurements off proton and deuteron targets. In the last line we report the total χ^2 and $\chi^2_{\rm d.o.f.}$ of the fit.

Experiment	χ^2	n. points	χ^2/points
Belle-z_1z_2 A_0^{UL}	14.0	16	0.88
Belle-z_1z_2 A_0^{UC}	13.6	16	0.85
BABAR-z_1z_2 A_0^{UL}	37.3	36	1.04
BABAR-z_1z_2 A_0^{UC}	13.0	36	0.36
BABAR-P_{1T} A_0^{UL}	5.6	9	0.63
BABAR-P_{1T} A_0^{UC}	3.1	9	0.35
Total A_0	86.7	122	0.71
HERMES p	31.6	42	0.75
COMPASS p	40.2	52	0.77
COMPASS d	58.5	52	1.12
Total SIDIS	130.3	146	0.89
Total	217.0	268	$\chi^2_{\rm d.o.f.} = 0.84$

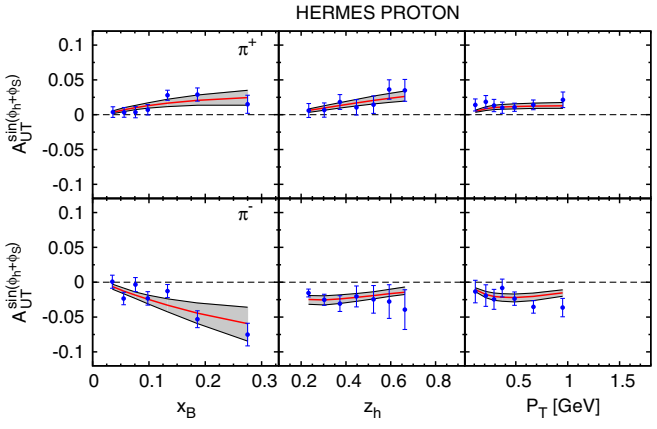

FIG. 1 (color online). The experimental data on the SIDIS azimuthal moment $A_{UT}^{\sin(\phi_h+\phi_S)}$ as measured by the HERMES Collaboration [4], are compared to the curves obtained from our global reference fit. The solid lines correspond to the parameters given in Table I, while the shaded areas correspond to the statistical uncertainty on these parameters, as explained in the text. Notice that, at order $k_\perp/Q$ and $p_\perp/Q$, $x_B = x$ and $z_h = z$.

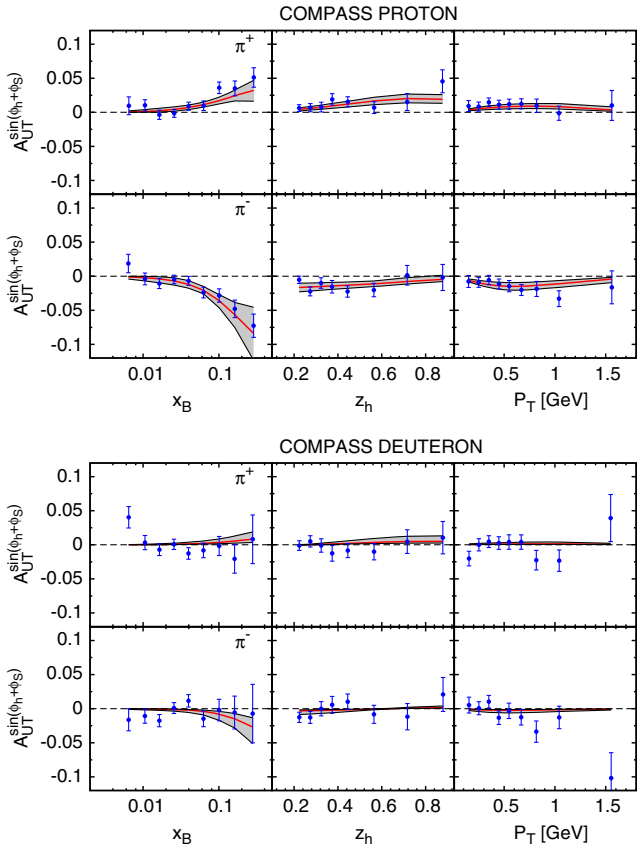

FIG. 2 (color online). The experimental data on the SIDIS azimuthal moment $A_{UT}^{\sin(\phi_h+\phi_S)}$ as measured by the COMPASS Collaboration on proton (upper panel) and deuteron (lower panel) targets [6,33], are compared to the curves obtained from our global reference fit. The solid lines correspond to the parameters given in Table I, while the shaded areas correspond to the statistical uncertainty on these parameters, as explained in the text. Notice that, at order $k_\perp/Q$ and $p_\perp/Q$, $x_B = x$ and $z_h = z$.

Figures 1 and 2 show our best-fit results for the azimuthal modulation $A_{UT}^{\sin(\phi_h+\phi_S)}$ as measured by the HERMES [4] and COMPASS [6,33] Collaborations in SIDIS processes, while Figs. 3 and 4 show our description of the azimuthal correlations A_0^{UL} and A_0^{UC}, as functions of z_1 and z_2 in unpolarized $e^+e^- \to h_1 h_2 X$ processes, measured by the Belle [31,32] and *BABAR* [12] Collaborations, respectively. Figure 5 shows our best fit of the *BABAR* A_0^{UL} and A_0^{UC} asymmetries as functions of P_{1T} (p_{t0} in the notation used by the *BABAR* Collaboration). We stress that these measurements offer the first direct insight of the dependence of the Collins function on the parton intrinsic transverse momentum: in fact, our global fit now delivers a more precise determination of the Gaussian width of the Collins function (through the M_C parameter, see Table I), which in our previous fits was affected by a very large uncertainty.

In Fig. 6 we show the valence quark transversity distributions and the lowest $\boldsymbol{p}_\perp$ moment of the favored and disfavored Collins functions as extracted from our reference fit, while in Fig. 7 we compare them with those extracted in our previous analysis [11]. Notice that, in the case of a factorized Gaussian shape, the lowest $\boldsymbol{p}_\perp$ moment of the Collins function,

$$\Delta^N D_{h/q^\uparrow}(z, Q^2) = \int d^2\boldsymbol{p}_\perp \Delta^N D_{h/q^\uparrow}(z, p_\perp, Q^2), \quad (39)$$

is related to the z-dependent part of the Collins function, $\tilde{\Delta}^N D_{h/q^\uparrow}(z, Q^2)$, Eqs. (6), (8) and (9), by the simple relation

$$\Delta^N D_{h/q^\uparrow}(z, Q^2) = \frac{\sqrt{\pi}}{2} \frac{\langle p_\perp^2 \rangle_C^{3/2}}{\langle p_\perp^2 \rangle} \frac{\sqrt{2e}}{M_C} \tilde{\Delta}^N D_{h/q^\uparrow}(z, Q^2). \quad (40)$$

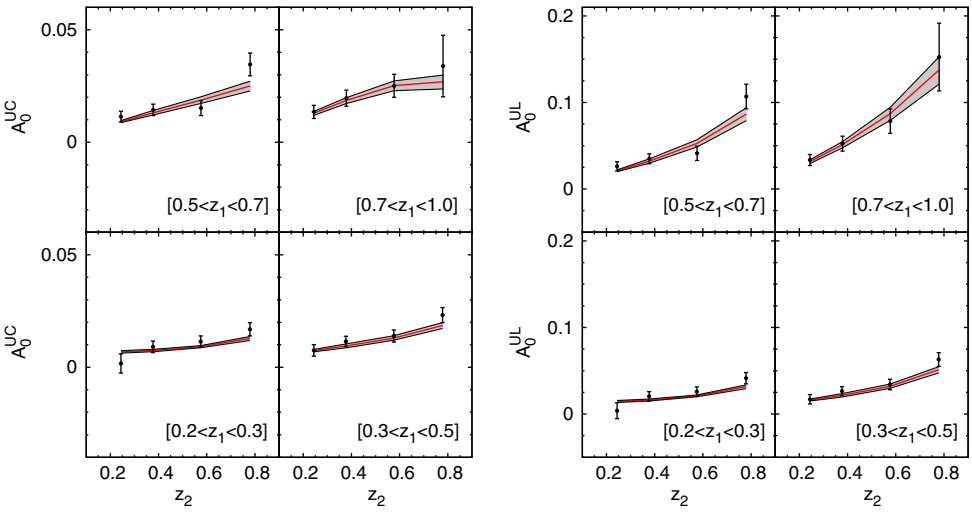

FIG. 3 (color online). The experimental data on the azimuthal correlations A_0^{UC} (left panel) and A_0^{UL} (right panel) as functions of z_1 and z_2 in unpolarized $e^+e^- \to h_1 h_2 X$ processes, as measured by the Belle Collaboration [31,32], are compared to the curves obtained from our global reference fit. The solid lines correspond to the parameters given in Table I, while the shaded areas correspond to the statistical uncertainty on these parameters, as explained in the text.

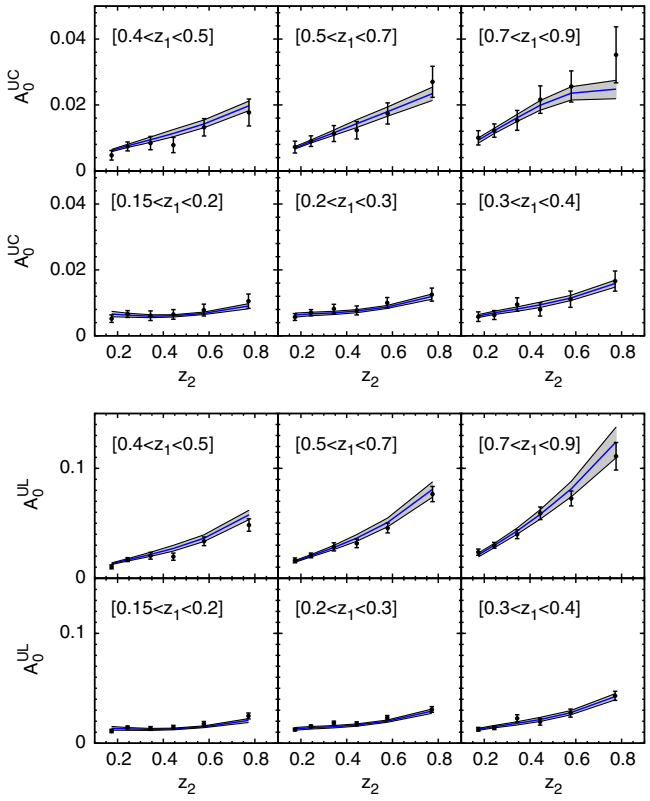

FIG. 4 (color online). The experimental data on the azimuthal correlations A_0^{UC} (upper panel) and A_0^{UL} (lower panel) as functions of z_1 and z_2 in unpolarized $e^+e^- \to h_1 h_2 X$ processes, as measured by the *BABAR* Collaboration [12], are compared to the curves obtained from our global reference fit. The solid lines correspond to the parameters given in Table I, while the shaded areas correspond to the statistical uncertainty on these parameters, as explained in the text.

In Figs. 6, 7 and 11 we plot $\Delta^N D_{h/q^\uparrow}(z, Q^2)$ in order to facilitate the comparison with the results of Refs. [9–11]. From Fig. 7 we can see that only the Collins functions differ significantly; this is due to the different choice of parametrization. In fact, given the lower statistics of the available data at that time, in 2013 we imposed that the favored and disfavored $\mathcal{N}^C(z)$ functions had the same z dependence and could differ only by a normalization constant, while in this paper, where we can count on a much higher statistics, they are left uncorrelated, with the disfavored function being simply a constant multiplied by the unpolarized fragmentation function [see Eqs. (11) and (12)]. The u_v and d_v transversity functions, instead, are well compatible with their u and d counterparts extracted in 2013. Notice that the present data actually allow the extraction of the sole u_v transversity function, due to the strong u dominance in the SIDIS data, while the d_v contribution remains highly underconstrained. We have checked that $\Delta_T d = 0$ is a possible solution (and it is in fact included in our uncertainty bands), and we cannot rule out a solution in which one would assume $\Delta_T d = -\frac{1}{4}\Delta_T u$ at a very low Q^2 scale, as inspired by a pure SU(6), nonrelativistic model. Moreover, for instance, one could consider a scenario with only u and $\bar{u}$ quark contributions, without any d transversity distribution, obtaining a best fit of comparable quality. This might have an important impact in the attempt to determine the tensor charge.

As mentioned above, in our global fit we include only the experimental e^+e^- measurements taken in the hadronic-plane reference frame, that is only the A_0^{UL} and A_0^{UC} asymmetries are used to constrain the model parameters. However, once the free parameters have been determined by the best-fit procedure, we can compare the predictions

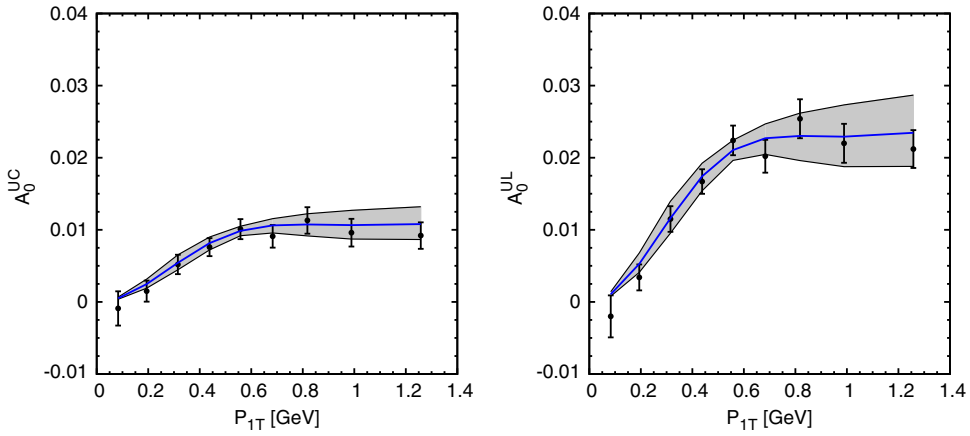

FIG. 5 (color online). The experimental data on the azimuthal correlations A_0^{UC} (left panel) and A_0^{UL} (right panel) as functions of P_{1T} in unpolarized $e^+e^- \to h_1 h_2 X$ processes, as measured by the *BABAR* Collaboration [12], are compared to the curves obtained from our global reference fit. The solid lines correspond to the parameters given in Table I, while the shaded areas correspond to the statistical uncertainty on these parameters, as explained in the text.

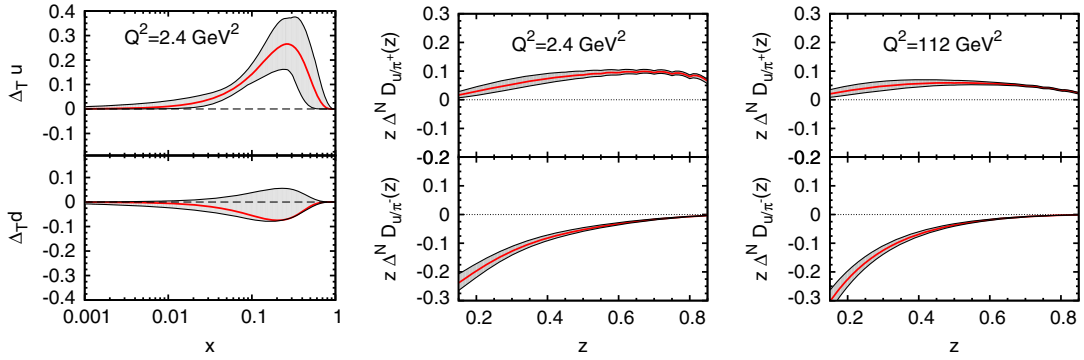

FIG. 6 (color online). Our best-fit results for the valence u and d quark transversity distributions at $Q^2 = 2.4$ GeV^2 (left panel) and for the lowest $\boldsymbol{p}_\perp$ moment of the favored and disfavored Collins functions at $Q^2 = 2.4$ GeV^2 (central panel) and at $Q^2 = 112$ GeV^2 (right panel). The solid lines correspond to the parameters given in Table I, while the shaded areas correspond to the statistical uncertainty on these parameters, as explained in the text.

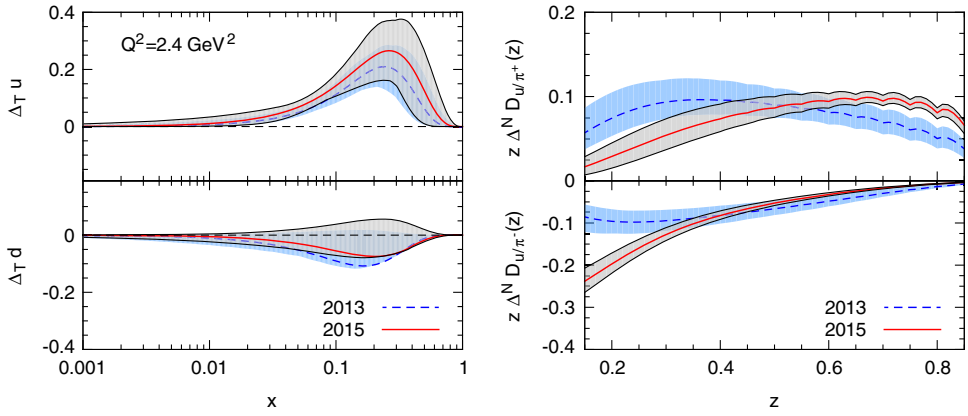

FIG. 7 (color online). Comparison of our reference best-fit results (red, solid lines) for the valence u and d quark transversity distributions (left panel) and for the lowest $\boldsymbol{p}_\perp$ moment of the favored and disfavored Collins functions (right panel), at $Q^2 = 2.4$ GeV^2, with those from our previous analysis [11] (blue, dashed lines).

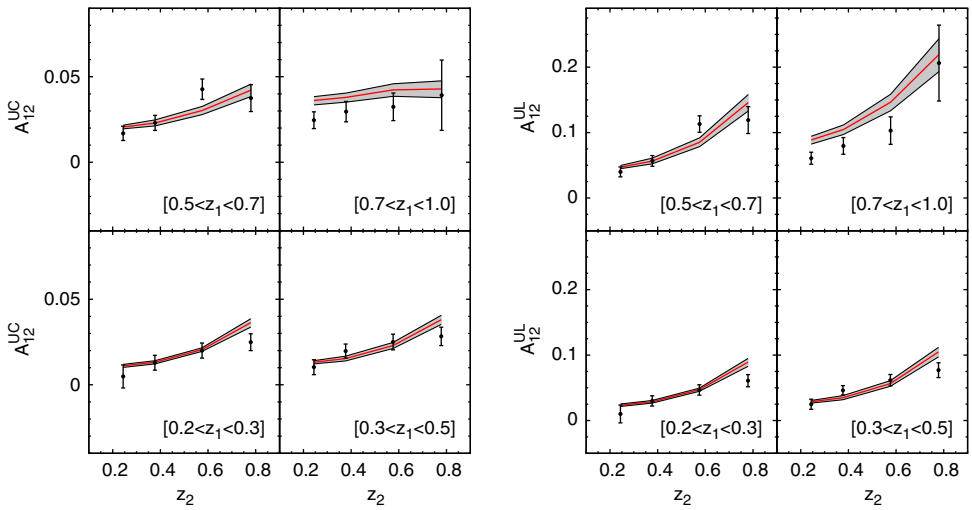

FIG. 8 (color online). The experimental data on the azimuthal correlations A_{12}^{UC} (left panel) and A_{12}^{UL} (right panel) as functions of z_1 and z_2 in unpolarized $e^+e^- \to h_1 h_2 X$ processes, as measured by the Belle Collaboration [31,32], are compared to the curves given by the parameters shown in Table I. The shaded areas correspond to the statistical uncertainty on these parameters, as explained in the text. These data have not been used in the global reference fit.

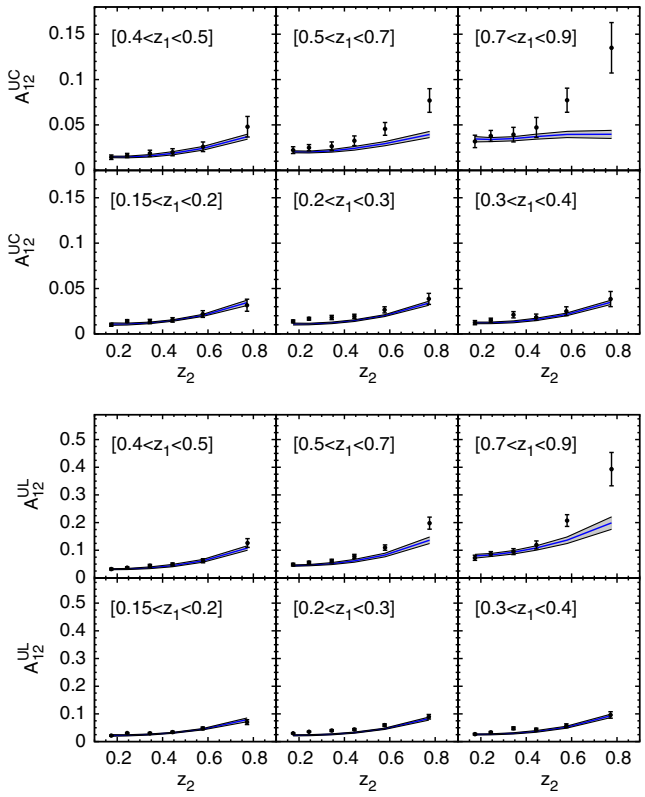

FIG. 9 (color online). The experimental data on the azimuthal correlations A_{12}^{UC} (upper panel) and A_{12}^{UL} (lower panel) as functions of z_1 and z_2 in unpolarized $e^+e^- \to h_1 h_2 X$ processes, as measured by the *BABAR* Collaboration [12] are compared to the curves given by the parameters shown in Table I. The shaded areas correspond to the statistical uncertainty on these parameters, as explained in the text. These data have not been used in the global reference fit.

obtained from our model with the measurements of the A_{12}^{UL} and A_{12}^{UC} asymmetries performed in the thrust-axis reference frame. Figs. 8–10 show this comparison: the predicted asymmetries are in satisfactory agreement with experimental data, even for the multidimensional azimuthal correlations (in bins of z_1, z_2, $p_{\perp 1}$ and $p_{\perp 2}$); there are only some problems with data points corresponding to large values of z_1 and z_2, but this is a delicate region where exclusive channels might contribute.

IV. ON THE ROLE OF ALTERNATIVE PARAMETRIZATIONS AND THE Q^2 EVOLUTION OF THE COLLINS FUNCTION

In Sec. III we performed a best fit by adopting a simple phenomenological Q^2 evolution for the Collins function: we assumed the ratio $\tilde{\Delta}^N D(z, Q^2)/D(z, Q^2)$ to be constant in Q^2, with the unpolarized fragmentation function $D(z, Q^2)$ evolving with a DGLAP kernel. However, the Collins function can be shown to be related to the collinear $H_{h/q}^{(3)}$ twist-three fragmentation function [42], the diagonal part of which evolves with a transversity kernel as the transversity function. Therefore, it is interesting to apply this kind of evolution to the Collins function and study the consequences of such an evolution on our best fit.

To this purpose, we assume the z-dependent part of the Collins distribution, $\tilde{\Delta}^N D_{h/q^\uparrow}$, to evolve with a transversity kernel, similarly to what is done for the transversity function, as suggested in Refs. [42,43]. The results we obtain show a slight deterioration of the fit quality, with a global $\chi^2_{\text{d.o.f.}}$ increasing from 0.84 to 1.20. Although this is still an acceptable result, one may wonder whether this is a genuine effect of the chosen evolution model or, rather, a byproduct of the functional form adopted for the Collins function parametrization.

We have therefore exploited a different parametrization based on a polynomial form. In principle, the polynomial could be of any order. We have started by using an order zero polynomial, then increased it to order one and, subsequently, to order two. In doing so, we have seen that the quality of the fit improves remarkably when going from order zero to order one (i.e. from two to four free parameters) but it stops improving when further increasing to higher orders. We therefore choose a first order polynomial form, which has the added advantage of depending on the same number of free parameters as the standard parametrization of Eqs. (11) and (12).

We consider generic combinations of fixed order Bernstein polynomials (see, for example, Ref. [44]) as they offer a relatively straightforward way to keep track of the appropriate normalization:

$$\mathcal{N}_i^C(z) = a_i P_{01}(z) + b_i P_{11}(z) \quad i = \text{fav}, \text{dis}, \quad (41)$$

where $P_{01}(z) = (1-z)$ and $P_{11}(z) = z$ are Bernstein polynomials of order one. Notice that by constraining the four free parameters in such a way that $-1 \le a_i \le +1$ and $-1 \le b_i \le +1$, the Collins function automatically fulfils its positivity bounds, as in the standard parametrization. The Collins function will be globally modeled as shown in Eqs. (6) and (8), with $\mathcal{N}_{\text{fav}}^C(z)$ and $\mathcal{N}_{\text{dis}}^C(z)$ as given in Eq. (41).

It turns out that with a transversitylike Q^2 evolution of the Collins function coupled to this polynomial parametrization, we can obtain best-fit results of similar quality as we found for our reference fit, with $\chi^2_{\text{d.o.f.}} = 1.00$. Notice that, adopting the polynomial parametrization and the standard evolution of the Collins function, one would obtain $\chi^2_{\text{d.o.f.}} = 0.92$ and no improvement would be achieved with respect to our reference fit.

In Table III we show the $\chi^2_{\text{d.o.f.}}$ corresponding to different choices of evolution and parametrization for the Collins functions. As it can be seen, all $\chi^2_{\text{d.o.f.}}$ are rather close to 1: this suggests that the observables we are fitting

FIG. 10 (color online). The experimental data on the multidimensional azimuthal correlations A_{12}^{UC} (upper panel) and A_{12}^{UL} (lower panel) in unpolarized $e^+e^- \to h_1 h_2 X$ processes, as measured by the *BABAR* Collaboration [12], are compared to the curves given by the parameters shown in Table I. The shaded areas correspond to the statistical uncertainty on these parameters, as explained in the text. These data have not been used in the global reference fit.

TABLE III. Values of $\chi^2_{\text{d.o.f.}}$ for different evolutions and parametrizations of the Collins function. Separate values for e^+e^- and SIDIS data are also given.

Evolution	Parametrization	χ^2/points e^+e^-	χ^2/points SIDIS	χ^2/d.o.f.
Standard	Standard	0.71	0.89	0.84
Standard	Polynomial	0.83	0.94	0.92
Transversity	Standard	1.17	1.15	1.20
Transversity	Polynomial	1.02	0.93	1.00

exhibit a very mild Q^2 dependence. In fact, we have checked that a similar $\chi^2_{\text{d.o.f.}}$ can be obtained by not including any Q^2 dependence at all in the PDFs and FFs. One of the reasons our model works well is that it allows for an approximate cancellation of the Q^2 dependence in the asymmetries.

Figure 11 shows a comparison between the Collins functions extracted from the same sets of data using the reference fit procedure (red, solid lines) and the transversitylike Q^2 evolution with a polynomial parametrization (blue, dashed lines). No really significant differences can be noticed. We do not show the same comparison between the transversity distributions obtained in the two best-fit procedures, as the differences would be hardly noticeable; this can be seen by comparing the values of the parameters $N^T_{u_v}, N^T_{d_v}, \alpha$ and β, fixing the transversity distributions, in Table I and IV.

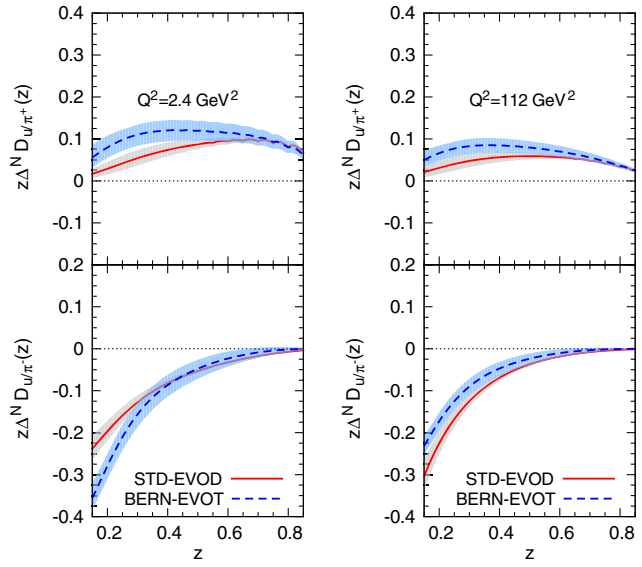

FIG. 11 (color online). Comparison of the lowest $\boldsymbol{p}_\perp$ moment, according to Eq. (39) of the text, of the favored (upper panels) and disfavored (lower panels) Collins functions at $Q^2 = 2.4$ GeV^2 (left panel) and at $Q^2 = 112$ GeV^2 (right panel) obtained from best-fit procedures using different evolution kernels and parametrizations. The solid red lines represent the Collins moments obtained by using the standard parametrization and employing the standard evolution. The dashed blue lines represent the same quantities obtained using the polynomial parametrization and by evolving the Collins function with a transversity kernel. The shaded areas correspond to the statistical uncertainty on the best-fit parameters, as explained in the text.

V. BESIII AZIMUTHAL CORRELATIONS

Quite recently, the BESIII Collaboration have released their measurements of the azimuthal Collins correlations in e^+e^- annihilations into pion pairs, completely analogous to those of *BABAR* and Belle, but at the lower energy $\sqrt{s} = Q = 3.65$ GeV [29]. BESIII has no clear jet event shape to help reconstructing the thrust axis (i.e. to separate hadrons coming from different fragmenting quarks or antiquarks). In fact, the BESIII Collaboration does not present A_{12}-type asymmetries. Instead, a cut on the opening angle (>120°) is required to select back-to-back pion pairs; the azimuthal correlations are then analyzed in the hadronic frame, as explained in Sec. II. We do not include these data in our fitting procedure. However, it is interesting to check the description of these new sets of measurements that our model can provide. Their low Q^2 values, as compared with Belle and *BABAR* experiments, might help in assessing the importance of TMD evolution effects.

In Fig. 12 the solid, black circles represent the A_0^{UC} and A_0^{UL} asymmetries measured by the BESIII Collaboration at $Q^2 = 13$ GeV^2, in bins of (z_1, z_2), while the solid blue circles (with their relative bands) correspond to the predictions obtained by using our reference fit results, presented in Sec. III. These asymmetries are well reproduced at small z_1 and z_2, where we expect our model to work, while they are underestimated at very large values of either z_1 or z_2, or both. Notice that the values of z_1, z_2 in the last bins are very large for an experiment with $\sqrt{s} = 3.65$ GeV: such data points might be affected by exclusive production contributions, and other effects which cannot be reproduced by a TMD model.

Figure 13 shows the same asymmetries, plotted as functions of P_{1T}. The A_0^{UC} asymmetry is described reasonably well by our model, while A_0^{UL} is slightly underestimated, especially at large P_{1T} where the effects of the experimental cuts, namely the opening angle, become more important.

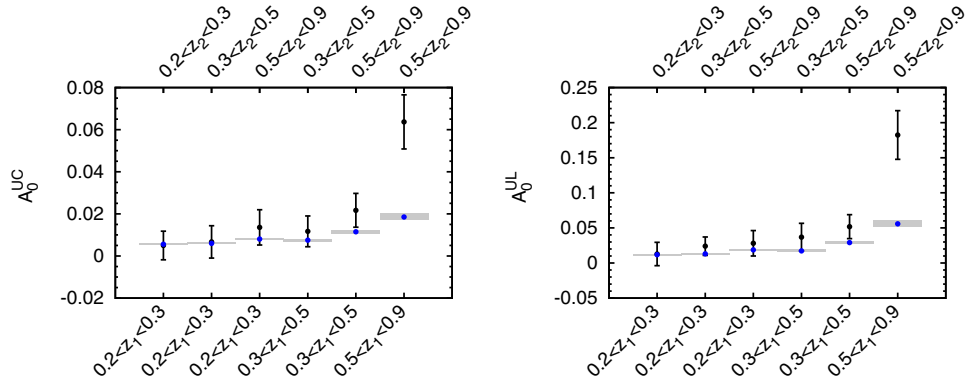

FIG. 12 (color online). The solid, black circles represent the A_0^{UC} (left panel) and A_0^{UL} (right panel) asymmetries measured by the BESIII collaboration at $Q^2 = 13$ GeV^2, in bins of (z_1, z_2) [29], while the solid blue circles (with their relative bands) correspond to the predictions obtained by using our reference fit results for the Collins functions.

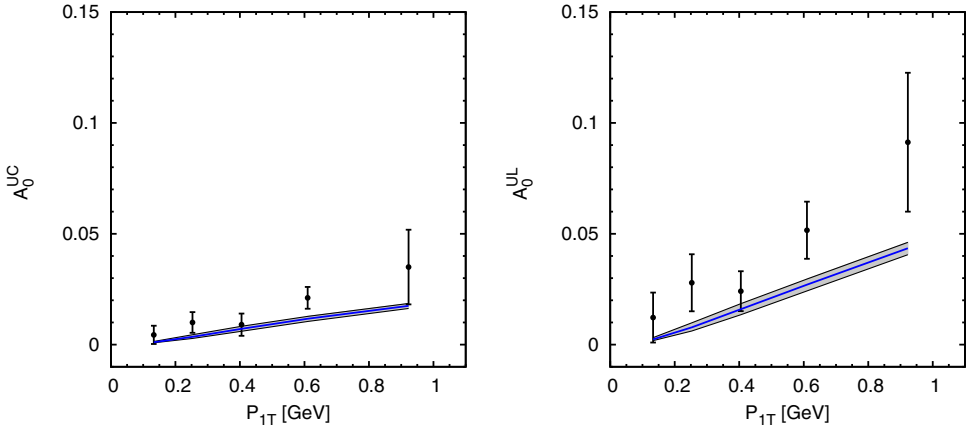

FIG. 13 (color online). The predictions obtained by using the Collins functions extracted from our reference fit of SIDIS ($Q^2 = 2 - 3$ GeV^2) and e^+e^- ($Q^2 = 112$ GeV^2) data (solid, blue lines) are compared to the A_0^{UC} (left panel) and A_0^{UL} (right panel) asymmetries measured by the BESIII collaboration [29] at $Q^2 = 13$ GeV^2, as functions of P_{1T} (black circles). The shaded areas on the theoretical curves correspond to the uncertainty on the parameters, as explained in the text.

Similar results, even with a slightly better agreement, are obtained using the results of our alternative fit, Table IV, based on a transversity evolution kernel for the Collins function combined with a polynomial parametrization. They are shown in Figs. 14 and 15.

At this stage, it is quite difficult to draw any clear-cut conclusion. The predictions of our approach, which does not include TMD evolution, seems to be quite satisfactory. On the other hand, the TMD evolution approach of Ref. [26] gives very good results. Despite the sizeable difference in Q^2 among the different sets of e^+e^- data, the measured asymmetries do not show any sensitivity to evolution effects in Q^2. Further comments will be given in the conclusions.

One should also add that, at the moderate energies of BESIII experiment, with the difficulties to isolate opposite jet hadrons, some corrections to the TMD factorized approach might still be relevant, like the appropriate insertion of kinematical cuts, of higher twist contributions and of threshold effects.

TABLE IV. Best-fit values of the nine free parameters fixing the u and d valence quark transversity distribution functions and the favored and disfavored Collins fragmentation functions, as obtained by fitting simultaneously SIDIS data on the Collins asymmetry and Belle and *BABAR* data on A_0^{UL} and A_0^{UC}, using the transversity kernel evolution and the polynomial parametrization.

$N^T_{u_v} = 0.58^{+0.42}_{-0.27}$	$N^T_{d_v} = -1.00^{+2.00}_{-0.00}$
$\alpha = 0.79^{+1.41}_{-0.62}$	$\beta = 1.44^{+7.92}_{-1.42}$
$a_{\rm fav} = -0.02^{+0.07}_{-0.09}$	$b_{\rm fav} = 0.66^{+0.14}_{-0.12}$
$a_{\rm dis} = -1.00^{+0.13}_{-0.00}$	$b_{\rm dis} = 0.12^{+0.38}_{-0.43}$
$M_C^2 = 0.27^{+0.17}_{-0.08}$ GeV^2	

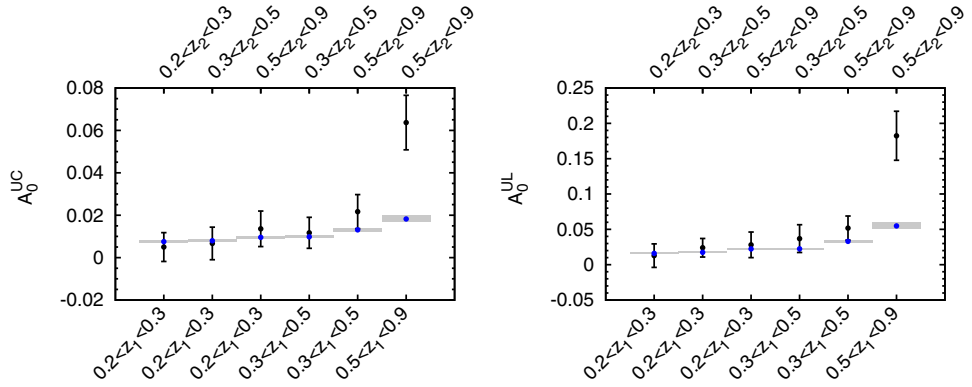

FIG. 14 (color online). The solid, black circles represent the A_0^{UC} (left panel) and A_0^{UL} (right panel) asymmetries measured by the BESIII collaboration [29] at $Q^2 = 13$ GeV^2, in bins of (z_1, z_2), while the solid blue circles (with their relative bands) correspond to the predictions obtained by using the Collins functions from our alternative fit, Table IV.

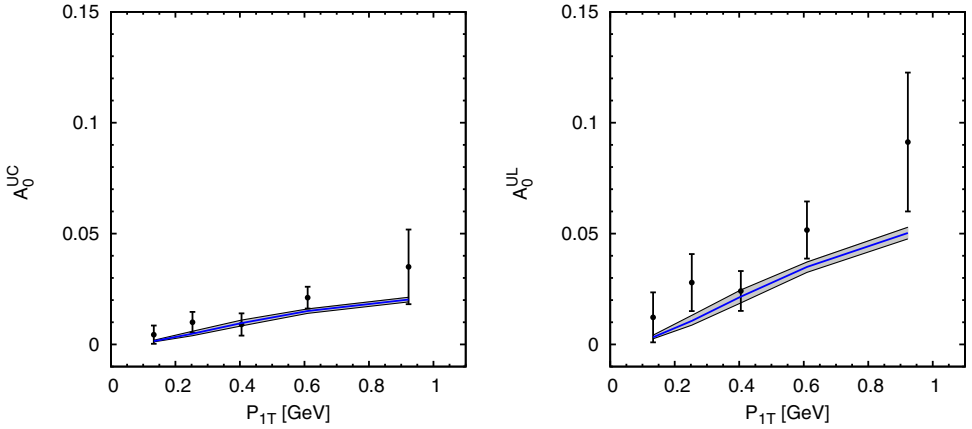

FIG. 15 (color online). The predictions obtained by using the Collins functions from our alternative fit, Table IV, (solid, blue lines) are compared to the A_0^{UC} (left panel) and A_0^{UL} (right panel) asymmetries measured by the BESIII Collaboration [29] at $Q^2 = 13$ GeV^2, as functions of P_{1T} (black circles). The shaded areas on the theoretical curves correspond to the uncertainty on the parameters, as explained in the text.

VI. COMMENTS AND CONCLUSIONS

We have performed a new global analysis of SIDIS and e^+e^- azimuthal asymmetries, motivated by the recent release of *BABAR* data, with high statistics and precision, which offer new insights on the $p_\perp$ dependence of the Collins azimuthal correlations A_0 and A_{12}. We have extracted the Collins functions and the transversity distributions by adopting a simple phenomenological model for these TMD–PDFs and FFs, such that their x- or z-dependent parts evolve with Q^2 while the transverse-momentum-dependent part is assumed to be Q^2 independent, i.e. by neglecting the TMD evolution.

The u and d quark transversity functions obtained by best-fitting SIDIS results and the new e^+e^- data simultaneously are compatible with the previous extractions [9–11]; while the u valence transversity distribution has a clear trend, the d valence transversity still shows large uncertainties. A similar procedure for the extraction of the transversity distributions, which combines SIDIS and e^+e^- data, involving the di-hadron fragmentation functions, has been adopted in Refs. [45–47]; the two methods obtain values of the transversity distributions which are well consistent with each other.

Instead, our newly extracted Collins functions look somewhat different from those obtained in our previous analyses. This is mainly due to the fact that we have exploited a different parametrization for the disfavored Collins function: while in the past we used a disfavored parametrization with the same shape of its favored counterpart, but with a different normalization (and sign), we have now modeled the disfavored Collins function independently. We have realized that one free parameter for the disfavored Collins function is enough to reach a fit of

excellent quality, indicating that the actual shape of the disfavored Collins function is still largely unconstrained by data.

About the $p_\perp$ dependence of the Collins function, we observe that its Gaussian width can now be determined with better precision. However, our extraction is still subject to a number of initial assumptions: a Gaussian shape for the TMDs, a complete separation between transverse and longitudinal degrees of freedom, a Gaussian width of the unpolarized TMD–FFs fixed solely by SIDIS data. Hopefully, higher statistics and higher precision multidimensional data, for asymmetries and unpolarized multiplicities, will help clarifying the picture.

We have also made an attempt to understand the Q^2 dependence of these experimental data. We see that our model provides a very satisfactory description of the data and, although it relies on a Q^2-independent $p_\perp$ distribution, the quality of our best fit is similar to that obtained by using TMD evolution [26]. This can be an indication that there might be cancellations of the Q^2 dependence of the TMDs in these azimuthal asymmetries, which are ratios or even double ratios of cross sections.

One can study these Q^2 evolution effects by directly comparing the same azimuthal correlations measured at very different Q^2 values by the *BABAR*-Belle and BESIII Collaborations. Our model predicts almost identical asymmetries for different Q^2. Differences among BESIII and *BABAR*-Belle asymmetries could be explained by the different kinematical configurations and cuts. Our predictions are in qualitatively good agreement with the present BESIII measurements, indicating that the data themselves do not show any strong sensitivity to the Q^2 dependence in the transverse momentum distribution. Also in this case, the predictions obtained from a TMD evolution approach can describe the data well: this points again to cancellations of the TMD evolution effects which occur in the ratios when computing the measured asymmetries.

We are thus led to believe that asymmetries or any observable which is constructed by taking ratios are not ideal grounds for the study of TMD evolution effects. More effort should be made towards measuring properly normalized SIDIS and e^+e^-, and Drell-Yan cross sections (both unpolarized and polarized) where details of TMD evolution might finally be unraveled.

ACKNOWLEDGMENTS

M. A., M. B., J. O. G. and S. M. acknowledge support from the "Progetto di Ricerca Ateneo/CSP" (codice TO-Call3-2012-0103). U. D. is grateful to the Department of Theoretical Physics II of the Universidad Complutense of Madrid for the kind hospitality extended to him during the completion of this work.

[1] D. W. Sivers, Phys. Rev. D **41**, 83 (1990).
[2] D. W. Sivers, Phys. Rev. D **43**, 261 (1991).
[3] J. C. Collins, Nucl. Phys. **B396**, 161 (1993).
[4] A. Airapetian *et al.* (HERMES Collaboration), Phys. Lett. B **693**, 11 (2010).
[5] C. Adolph *et al.* (COMPASS Collaboration), Phys. Lett. B **717**, 376 (2012).
[6] C. Adolph *et al.* (COMPASS Collaboration), Phys. Lett. B **744**, 250 (2015).
[7] D. Boer, R. Jakob, and P. Mulders, Nucl. Phys. **B504**, 345 (1997).
[8] K. Abe *et al.* (Belle Collaboration), Phys. Rev. Lett. **96**, 232002 (2006).
[9] M. Anselmino, M. Boglione, U. D'Alesio, A. Kotzinian, F. Murgia, A. Prokudin, and C. Türk, Phys. Rev. D **75**, 054032 (2007).
[10] M. Anselmino, M. Boglione, U. D'Alesio, A. Kotzinian, F. Murgia, A. Prokudin, and S. Melis, Nucl. Phys. B, Proc. Suppl. **191**, 98 (2009).
[11] M. Anselmino, M. Boglione, U. D'Alesio, S. Melis, F. Murgia, and A. Prokudin, Phys. Rev. D **87**, 094019 (2013).
[12] J. Lees *et al.* (*BABAR* Collaboration), Phys. Rev. D **90**, 052003 (2014).
[13] P. Schweitzer, T. Teckentrup, and A. Metz, Phys. Rev. D **81**, 094019 (2010).
[14] M. Anselmino, M. Boglione, J. Gonzalez Hernandez, S. Melis, and A. Prokudin, J. High Energy Phys. 04 (2014) 005.
[15] A. Signori, A. Bacchetta, M. Radici, and G. Schnell, J. High Energy Phys. 11 (2013) 194.
[16] M. Anselmino, M. Boglione, U. D'Alesio, A. Kotzinian, S. Melis, F. Murgia, A. Prokudin, and C. Turk, Eur. Phys. J. A **39**, 89 (2009).
[17] M. Anselmino, M. Boglione, and S. Melis, Phys. Rev. D **86**, 014028 (2012).
[18] M. Anselmino, M. Boglione, U. D'Alesio, E. Leader, S. Melis, F. Murgia, and A. Prokudin, Phys. Rev. D **86**, 074032 (2012).
[19] M. Anselmino, M. Boglione, U. D'Alesio, S. Melis, F. Murgia, and A. Prokudin, Phys. Rev. D **88**, 054023 (2013).
[20] J. C. Collins, *Foundations of Perturbative QCD* (Cambridge University Press, Cambridge, England, 2011).
[21] J. C. Collins and D. E. Soper, Nucl. Phys. **B193**, 381 (1981); **B213**, 545(E) (1983).
[22] J. C. Collins and D. E. Soper, Nucl. Phys. **B194**, 445 (1982).
[23] S. M. Aybat and T. C. Rogers, Phys. Rev. D **83**, 114042 (2011).

[24] M. G. Echevarria, A. Idilbi, A. Schafer, and I. Scimemi, Eur. Phys. J. C **73**, 2636 (2013).
[25] M. G. Echevarria, A. Idilbi, and I. Scimemi, Phys. Rev. D **90**, 014003 (2014).
[26] Z.-B. Kang, A. Prokudin, P. Sun, and F. Yuan, arXiv:1505.05589.
[27] C. A. Aidala, B. Field, L. P. Gamberg, and T. C. Rogers, Phys. Rev. D **89**, 094002 (2014).
[28] J. Collins and T. Rogers, Phys. Rev. D **91**, 074020 (2015).
[29] M. Ablikim *et al.* (BESIII Collaboration), arXiv:1507.06824.
[30] B. Aubert *et al.* (*BABAR* Collaboration), arXiv:1506.05864.
[31] R. Seidl *et al.* (Belle Collaboration), Phys. Rev. D **78**, 032011 (2008).
[32] R. Seidl *et al.* (Belle Collaboration), Phys. Rev. D **86**, 039905(E) (2012).
[33] M. Alekseev *et al.* (COMPASS), Phys. Lett. B **673**, 127 (2009).
[34] M. Anselmino, M. Boglione, U. D'Alesio, S. Melis, F. Murgia, E. R. Nocera, and A. Prokudin, Phys. Rev. D **83**, 114019 (2011).
[35] A. Bacchetta, M. Diehl, K. Goeke, A. Metz, P. J. Mulders, and M. Schlegel, J. High Energy Phys. 02 (2007) 093.
[36] A. Bacchetta, U. D'Alesio, M. Diehl, and C. A. Miller, Phys. Rev. D **70**, 117504 (2004).
[37] M. Gluck, E. Reya, and A. Vogt, Eur. Phys. J. C **5**, 461 (1998).
[38] D. de Florian, R. Sassot, and M. Stratmann, Phys. Rev. D **76**, 074033 (2007).
[39] J. Pumplin, D. R. Stump, J. Huston, H. L. Lai, P. M. Nadolsky, and W. K. Tung, J. High Energy Phys. 07 (2002) 012.
[40] G. P. Salam and J. Rojo, Comput. Phys. Commun. **180**, 120 (2009).
[41] M. Gluck, E. Reya, M. Stratmann, and W. Vogelsang, Phys. Rev. D **63**, 094005 (2001).
[42] F. Yuan and J. Zhou, Phys. Rev. Lett. **103**, 052001 (2009).
[43] Z.-B. Kang, Phys. Rev. D **83**, 036006 (2011).
[44] R. T. Farouki, Computer Aided Geometric Design **29**, 379 (2012).
[45] A. Bacchetta, A. Courtoy, and M. Radici, Phys. Rev. Lett. **107**, 012001 (2011).
[46] A. Courtoy, A. Bacchetta, M. Radici, and A. Bianconi, Phys. Rev. D **85**, 114023 (2012).
[47] A. Bacchetta, A. Courtoy, and M. Radici, J. High Energy Phys. 03 (2013) 119.